PERGAMON

Radiation Measurements 32 (2000) 181–191

Radiation Measurements

www.elsevier.com/locate/radmeas

Analysis of MIR-18 results for physical and biological dosimetry: radiation shielding effectiveness in LEO

F.A. Cucinotta[a,*], J.W. Wilson[b], J.R. Williams[c], J.F. Dicello[c]

[a]*NASA, Johnson Space Center, Houston, TX 77058, USA*
[b]*NASA, Langley Research Center, Hampton, VA 86581, USA*
[c]*The Oncology Center, Johns Hopkins Medical School, Baltimore, MD 21287, USA*

Received 8 March 1999; received in revised form 8 May 1999; accepted 22 October 1999

Abstract

We compare models of radiation transport and biological response to physical and biological dosimetry results from astronauts on the Mir space station. Transport models are shown to be in good agreement with physical measurements and indicate that the ratio of equivalent dose from the Galactic Cosmic Rays (GCR) to protons is about 3/2:1 and that this ratio will increase for exposures to internal organs. Two biological response models are used to compare to the Mir biodosimetry for chromosome aberration in lymphocyte cells; a track-structure model and the linear-quadratic model with linear energy transfer (LET) dependent weighting coefficients. These models are fit to in vitro data for aberration formation in human lymphocytes by photons and charged particles. Both models are found to be in reasonable agreement with data for aberrations in lymphocytes of Mir crew members: however there are differences between the use of LET dependent weighting factors and track structure models for assigning radiation quality factors. The major difference in the models is the increased effectiveness predicted by the track model for low charge and energy ions with LET near 10 keV/μm. The results of our calculations indicate that aluminum shielding, although providing important mitigation of the effects of trapped radiation, provides no protective effect from the galactic cosmic rays (GCR) in low-earth orbit (LEO) using either equivalent dose or the number of chromosome aberrations as a measure until about 100 g/cm^2 of material is used. Published by Elsevier Science Ltd.

1. Introduction

The use of in vivo biological assays (biodosimetry) to study space radiation exposures to the astronauts can serve several purposes including verification of doses received, validation of risk methodologies, and the study of mechanisms of radiation effects. Biological assays include scoring chromosome aberrations in lymphocytes (Edwards, 1997), the use of serial activation of gene expression (SAGE) (Velculescu et al., 1995), protein expression including kinase activity, and measurements of the fraction of apoptotic cells (Menz et al., 1997). The observation of chromosome aberrations in lymphocyte cells extracted from blood samples is a convenient marker of radiation response which has a proven resolution for exposures above a few cGy (Edwards, 1997). The longer missions on the Russian Space Station Mir and those scheduled for the International Space Station (ISS) allow studies of chromosome aberration formation to be performed using a practical number of cells for the first time. Testard et

* Corresponding author. Fax: +1-281-483-5276.

1350-4487/00/$ - see front matter Published by Elsevier Science Ltd.
PII: S1350-4487(99)00273-5

al. (1996), Yang et al. (1997), and Obe et al. (1997) have studied chromosome aberration formation in lymphocytes from Mir crew members providing human in vivo data to test models. In this paper, we present calculations using the HZETRN radiation transport (Cucinotta et al., 1996; Wilson et al., 1991) and two biological response models which are compared to the Mir-18 results for chromosome aberration formation. We use these comparisons to discuss the role of biological response models and shielding effectiveness in low earth orbit (LEO).

Radiation sources in LEO include contributions from trapped protons and electrons, galactic cosmic rays (GCR), and sporadic exposures from solar particle events. The energy spectrum of each source determines their range in shielding material and the human body. Trapped electron energies extend to a few MeV with ranges of 1–2 cm in water and include a small bremmstrahlung component capable of reaching larger depths. Trapped protons have energies extending to several hundred MeV, however more than 90% of the flux is from particles with ranges less than 1 cm in water. A small high-energy component is capable of penetrating crew compartments and tissues producing nuclear secondaries including neutrons and highly ionizing hydrogen, helium, and heavy ions (Cucinotta et al., 1996a). In contrast to trapped radiation, incident GCR in LEO are dominated by relativistic particles with energies of 1 GeV/amu or more since the Earth's magnetic field provides shielding from the lower energy components (Cucinotta et al., 1995, 1996a). Relativistic ions have large ranges in matter and undergo numerous nuclear reactions in shielding and a large build-up of secondary particles including neutrons, hydrogen and helium ions, heavy ions, and mesons will occur inside spacecraft and tissues. The diverse nature of radiation components and the fact that few radiobiological data exist for these components place a large uncertainty in the assignment of radiation weighting factors. The material dependence of radiation component modulation and the large uncertainty in their effectiveness leaves the effectiveness of shielding in LEO poorly understood.

We consider two biophysical models for aberrations in this report; the linear-quadratic (LQ) model with linear energy transfer (LET) dependent weighting coefficients and a track structure model of cellular damage. It is in common practice to define radiation quality in terms of LET. Energy deposition at the cellular level is poorly described by LET because of the poor correlation of LET with energy deposition in microscopic targets such as DNA and the heterogeneity of energy deposition in individual cells. Track structure models provide descriptions of energy deposition in biological target molecules (Charlton et al., 1989; Cucinotta et al., 1995; Nikjoo et al., 1997). The two models considered herein are fit to in vitro data for aberration formation in human lymphocytes and combined with models of the space radiation environment and the HZETRN transport code to compare to the Mir-18 in vivo data. Other biological factors in low dose-rate exposures that should be addressed in order to understand space biodosimetry will be considered elsewhere.

2. Radiation transport methods

The Boltzmann equation considers atomic and nuclear reaction processes in the propagation of a boundary source of particles through shielding in order determine the particle flux, ϕ_j (x,E), of ion j with energy, E and depth, x (Wilson et al., 1991)

$$\Omega \cdot \nabla \phi_j(x, \Omega, E) = \Sigma_k \int \sigma_{jk}(\Omega, \Omega', E, E')\phi_k(x, \Omega', E')\mathrm{d}E'\mathrm{d}\Omega' - \sigma_j(E)\phi_j(x, \Omega, E) \quad (1)$$

In solving Eq. (1) the HZETRN/BRYNTRN code uses the straight-ahead and continuous slowing down (csda) approximations. The inclusive cross sections for absorption, σ_j, and fragmentation, knock-out elastic scattering etc., σ_{jk}, are described elsewhere (Wilson et al., 1991). The cross sections for nuclear fragmentation are from the QMSFRG model which has shown good agreement with experiments (Cucinotta et al., 1998).

2.1. Conventional risk assessment

Conventional risk assessment uses dose-based concepts to relate the macroscopic dose and the rate of energy loss per unit path-length (LET) of a particle to cancer mortality risk through a LET-dependent weighting factor and tissue specific risk coefficients. The equivalent dose-rate is defined for a single radiation component (NCRP, 1989)

$$H_T = \phi_T L Q(L) \quad (2)$$

where ϕ_T is the particle flux at the tissue site, L the LET, and Q the quality factor. For mixed radiation fields the total dose equivalent at depth, x is found by summing over all radiation components as

$$H_T = \Sigma_j \int \mathrm{d}E \phi_j(x, E) L(E) Q[L(E)] \quad (3)$$

The risk of cancer mortality is found by multiplying the dose equivalent by an appropriate risk coefficient estimated from cancer induction in humans from gamma-ray exposures. The resulting algorithm relates the risk per Sv to cancer mortality for a specific tissue (NCRP, 1989) as

$$\text{Risk} = R_0 H_T \quad (4)$$

Fig. 1 shows the dependence of Q on LET as recommended by ICRP-60 (1990), ICRP-26 (1976), and the Russian standard (GOST, 1991). This comparison shows the differences seen in the definition of radiation quality by various commissions and their evolution with time. Each of these regulatory bodies have used LET as the physical descriptor of the radiation field largely because of lack of information to define a more precise relationship of radiation quality. Neutron weighting factors are defined as a function of neutron energy. Unfortunately, space radiation exposures are more diverse in comparison to environmental exposures of concern to regulatory bodies: photons, radon gas, or reactor neutrons. The broad distribution in particle energies, charges, and LETs that occurs in space (Wilson et al., 1991) suggests a large uncertainty in the prescription of a Q vs LET relation. Such uncertainties are broadened by the distribution of tissue sensitivities where a unique Q relation is unlikely to be well founded.

In Fig. 2 we show calculations of the attenuation of the dose and dose equivalent in the Mir orbit (51.6 deg by 390 km) for 1997 in aluminum, water, polyethylene, and liquid hydrogen shielding. For the dose equivalent comparisons, the large differences between the lower mass materials and aluminum show the protective effects that occur through reduction of nuclear secondary production. Important physical processes in the use of material selection in the control of secondary radiation is the production of light fragments from target atoms, such as neutrons, protons, and alpha particles, and more efficient fragmentation of heavy ions by lower mass target atoms. These effects have been discussed in a space exploration context several times in the past (Cucinotta and Wilson, 1997; Letaw et al., 1989; Wilson et al., 1995). The comparison in Fig. 2b shows that the role of material selection in mitigating the effects of the GCR is more pronounced in LEO in comparison to previous calculations in free space (Cucinotta and Wilson, 1997; Letaw et al., 1989; Wilson et al., 1995). Here an amplification of the importance of nuclear reactions occurs due to the Earth's magnetic field filtering the entry of low and medium energy GCR components into LEO, since nuclear mean free paths reach a maximum for relativistic ions. Fig. 3 shows for aluminum shielding, the contributions from different charge groups, including heavy-ion recoils produced from neutrons. Large modulation in dominant ion contributors occurs as the amount of shielding is increased; however, following an initial build-up of secondaries at the shield entrance, the overall response obtains only a slow attenuation. Fig. 4 shows the attenuation of the trapped proton contributions behind aluminum, water, polyethylene, and

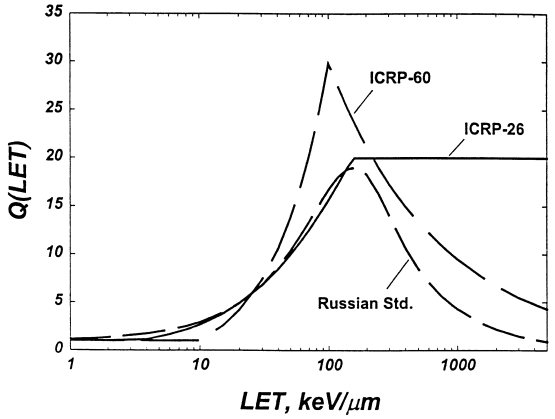

Fig. 1. Radiation quality factors vs LET as assigned by several regulating bodies.

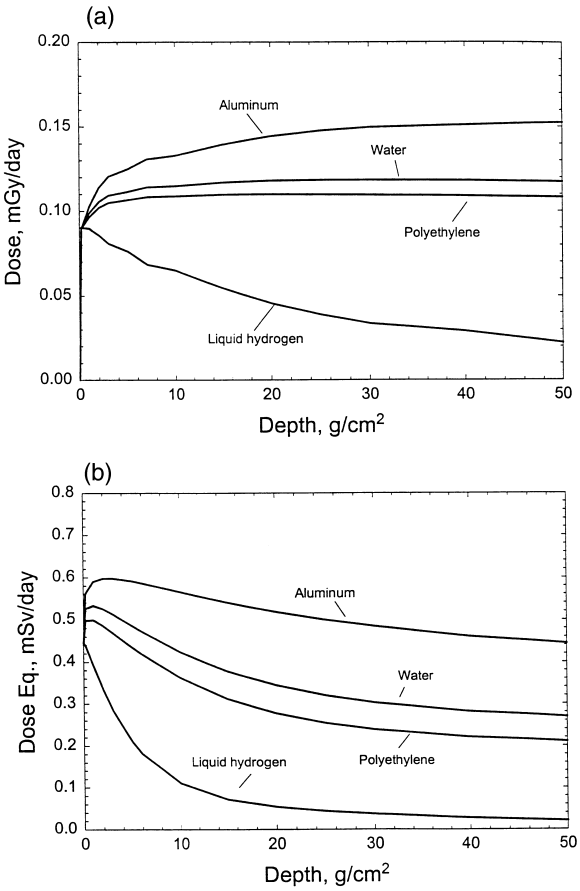

Fig. 2. (a) Comparison of calculations of the absorbed dose vs shielding thickness for several materials from GCR in 51.6 deg × 390 km orbit. (b) Comparison of calculations of the dose equivalent vs shielding thickness for several materials from GCR in 51.6 deg × 390 km orbit.

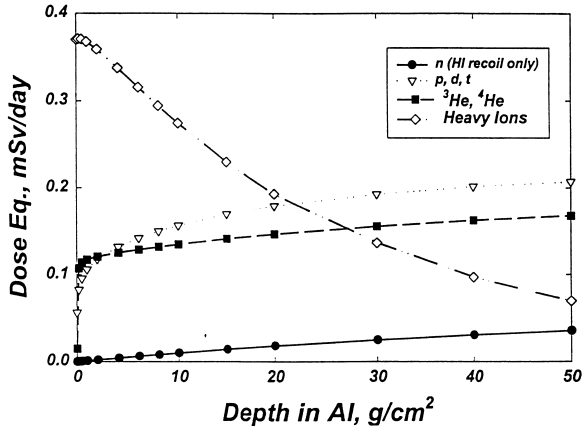

Fig. 3. Contributions over different charge groups vs depths from GCR in aluminum.

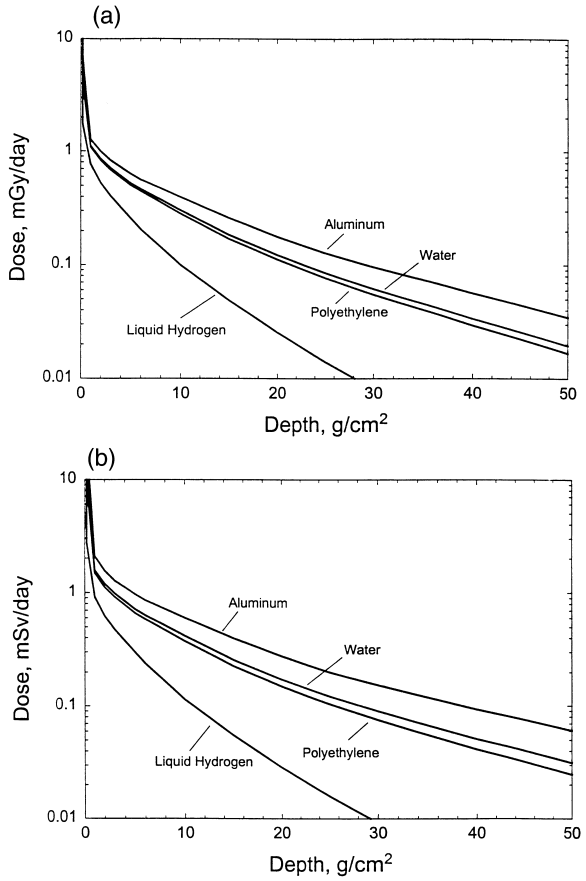

Fig. 4. (a) Comparison of calculations of the absorbed dose vs shielding thickness for several materials from trapped protons in 51.6 deg × 390 km orbit. (b) Comparison of calculations of the dose equivalent vs shielding thickness for several materials from trapped protons in 51.6 deg × 390 km orbit.

liquid hydrogen shielding. Clearly, material composition is important in estimating the radiation transport properties of proton exposures as well as the GCR. About 50% of the dose equivalent at large depths is from nuclear secondaries for the case of aluminum shielding (Cucinotta et al., 1996a) and this fraction is significantly reduced for materials with lower mass constituents.

The HZETRN code has been used to compare to LEO measurements several times in the past (Badhwar and Cucinotta, 1998; Cucinotta et al., 1995). Good agreement with active measurements of the GCR are observed (Badhwar et al., 1998); however, these comparisons are made directly to data uncorrected for their ion response efficiency. Table 1 shows comparisons of HZETRN to the uncorrected data from a tissue equivalent proportional counter (TEPC) on Mir-18 for dose- and dose-equivalent rates. Calculations are shown at two locations inside the Mir station, denoted as Naussica and Lluyin. The corresponding mass distributions are shown in Fig. 5. In Badhwar et al. (1998) it was noted that the TEPC was flown at a location with about 4 g/cm^2 more shielding than the Naussica location. This comparison is also shown in Table 1 and is in reasonable agreement with the TEPC data. The AP8 trapped proton environmental model is often quoted to be uncertain by up to a factor of 2 in predicting doses (Badhwar et al., 1998). The comparison shown in Table 1 indicates that most likely this in an upper bound for the Mir-18 mission. The ratio of dose equivalent contributions from GCR to trapped protons is about 3/2:1 and this ratio will increase for exposures to internal organs.

The comparisons in Figs 2–4 and Table 1 have several important consequences. First, radiation transport codes that exclude a description of nuclear reactions do not accurately describe the effects of space radiation

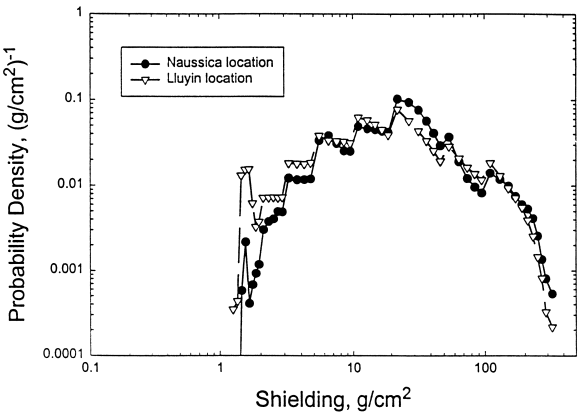

Fig. 5. The fractional contribution of aluminum shielding thickness on the Mir station at the Lyulin and Naussica locations.

including trapped protons and solar particle events (Cucinotta et al., 1996a), as well as the GCR. Second, aluminum shielding provides no protective effect from the GCR in LEO until about 100 g/cm^2 of material is used (result not shown). Current shielding models which employ an 'effective aluminum' depth by summing the mass distribution from diverse materials contained on-board spacecraft (water storage, foods, plastics) do not provide an adequate approximation for calculating the secondary radiation. The present results indicate that such approximations may introduce a significant error in methods used to predict organ doses. These findings have important implications for the design of new modules for the ISS such as the Transhab that use lighter mass constituents for radiation materials. Finally, previous studies have shown that alternative risk methodologies differ substantially with LET dependent quality factors or weighting factors in estimating the effectiveness of space radiation shielding (Cucinotta and Wilson, 1997; Letaw et al., 1989; Wilson et al., 1995). A study of biodosimetry results for possible verification of these earlier findings is discussed next.

3. Biophysical risk models

We next discuss two biophysical response models that allow ground-based radiobiology data for chromosome aberrations to be used with environmental models and radiation transport codes to predict responses in spaceflight. The two models discussed are based on distinct models of energy deposition and methods of extrapolation of the dose response as a function of radiation quality from in vitro data.

3.1. LET model for chromosome aberrations

Common models of chromosome aberration formation include the classical model and the exchange models (Revell, 1974; Sachs et al., 1997; Savage, 1989). Briefly, these models relate the formation of pairs of double strand breaks (DSB) or other lesion pairs that interact and mis-join to the formation of specific chromosome aberrations. These models can include descriptions of microscopic energy deposition in cells or the role of chromosome geometry (Chen et al., 1997; Edwards et al., 1994). A criticism of these models is that they largely ignore the role of biological process such as homologous or non-homologous recombination (Resnick, 1976; Roth et al., 1985), enzymatic processing of breaks (Nelson and Kastan, 1994; Reed et al., 1995), and signal transduction processes (Morgan et al., 1996). The role of V(J)D recombination in lymphocyte cells is well established (Alt et al., 1992; Friedberg et al., 1995). In recombination models of DSB repair (Resnick, 1976; Roth et al., 1985), chromosome aberrations form from isolated breaks through mis-joining of DNA structures that proceed from recombinatory intermediates such as Holiday junctions or D-loops. There will continue to be a considerable uncertainty in risk models that preclude a role for established processes that control DNA damage processing including the formation of chromosome aberrations.

The exchange or classical models of aberration formation can be expressed in terms of a linear-quadratic function of absorbed dose as given by (Edwards et al., 1994; Sachs et al., 1997)

$$N_{\text{aber}} = \alpha D + \beta(t) D^2 \tag{5}$$

where the linear coefficient, α, is assumed to be independent of dose-rate, and the quadratic component, β, contains a dependency on irradiation time to describe the reduction in the number of aberrations with decreasing dose rate. For exposures in space, dose-rates are sufficiently small such that the second term in Eq. (5) can be ignored. The α-coefficient is assumed to be proportional to LET up to a maximum value and to decline at values above about 100 keV/μm due to the effects of over-kill or interphase cell death (Edwards et al., 1994). Using this approach we have fit

Table 1
Comparisons of calculations and measurements [18] for dose- and dose-equivalent rate on Mir-18

	GCR			Trapped protons			Total		
	Dose (mGy/day)	Dose equivalent (mSv/day)	Q	Dose (mGy/day)	Dose equivalent (mSv/day)	Q	Dose (mGy/day)	Dose equivalent (mSv/day)	Q
TEPC	0.142	0.461	3.2	0.153	0.298	1.9	0.295	0.759	2.6
Model:									
Naussica	0.138	0.535	3.9	0.191	0.295	1.5	0.329	0.830	2.5
Naussica[a] +4 g/cm^2	0.141	0.526	3.7	0.140	0.219	1.6	0.281	0.745	2.7
Lyulin	0.134	0.547	4.1	0.254	0.391	1.5	0.388	0.938	2.4

[a] The TEPC shielding was close to this distribution on Mir-18.

the α-coefficient for the formation of dicentrics in Fig. 6 to available charged particle data (Edwards, 1997; Edwards et al., 1994; Sasaki et al., 1998). This model is qualitatively similar to the $Q(L)$ relation defined by the ICRP (ICRP-60, 1990). Of note is that biological response is assumed to be independent of the charge or velocity of an ion, despite much experimental evidence to the contrary (e.g., Belli et al., 1993, 1994; Kiefer and Schneider, 1994; Thacker et al., 1979), and the findings of other biophysical models (Charlton et al., 1989; Katz et al., 1971). However, a simple LET dependence is often invoked because of the lack of the number of experimental values for different ion types to determine a more detailed functional behavior. Edwards et al. (1994) has developed a response function based on the lineal energy, y deposited in a 1 μm sphere as an alternative to the use of LET.

3.2. Track model of chromosome aberrations

We next discuss the use of the average track model to describe aberration formation in human lymphocytes. The model uses a mapping procedure to correlate the dose-response for aberration formation from acute electron or photon exposures to the microscopic distribution of energy about the path of an ion (Cucinotta et al., 1996b; Katz et al., 1971). In this way, assumptions on the mechanism of aberration are largely avoided. In the average-track model the probability of a cell not receiving an aberration from an acute photon exposure is written

$$P(D) = \exp(-n_{\mathrm{aber}}(D)) \tag{6}$$

where n_{aber} is the number of aberrations formed in the exposure. The following functional form provides a good representation of the photon data,

$$P(D) = 1 - \exp(-\alpha_\gamma D)(1 - (-D/D_0)^m) \tag{7}$$

where α_γ is the linear-coefficient of the gamma-ray response with the value of 0.2 Gy^{-1} (Edwards, 1997), and D_0 and m are parameters values found as $D_0 = 2$ Gy and $m = 3$.

The average number of aberrations per cell is found from Eq.(6) as

$$n_{\mathrm{aber}} = -\log(P(D)) \tag{8}$$

In considering the effects of ions, the average track model uses the dose-response from x-rays or gamma-rays as a mapping function that is combined with the radial distribution of energy deposition about the ions path to predict the effects of an ion at radial distance, b from a biological target. The radial distribution falls off as $1/b^2$ reaching doses of 10^6–10^9 Gy close to the ion track and dependent on the square of the ion charge. Summation of contributions from all radial distances yields the biological action cross section of the ion. The radial distance of the ion to a biological target is restricted by the maximum range of δ-rays which is a function of ion velocity. The action cross section for aberration formation from ion, j with energy, E is given by

$$\sigma_j(E) = 2\pi \int b\, \mathrm{d}b \quad P[D_{\mathrm{ave}}(j, E, b)] \tag{9}$$

where $D_{\mathrm{ave}}(j,E,b)$ is the radial distribution of energy deposition by an ion averaged over the area of the target volume assumed to be a short cylinder of radius 0.5 μm in the calculations, however for the linear-term in $P(D)$ [Eq. (7)] we use a smaller site-size representing a short DNA segment of 2 nm. The response for ions is then written (Cucinotta et al., 1996b; Katz et al., 1971) as

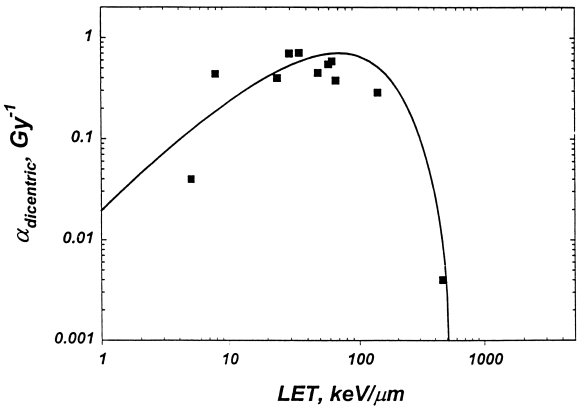

Fig. 6. Comparison of L–Q LET model for initial slopes to experimental data for dicentrics in human lymphocytes (Edwards, 1997; Edwards et al., 1994; Sasaki et al., 1998).

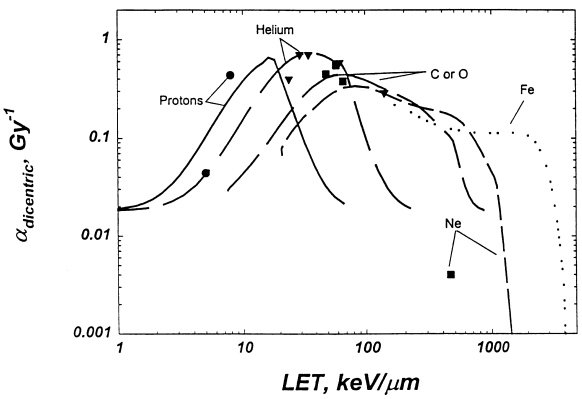

Fig. 7. Comparison of track model for initial slopes to experimental data for dicentrics in human lymphocytes (Edwards, 1997; Edwards et al., 1994; Sasaki et al., 1998).

Table 2
Comparisons of calculations to measurements for fraction of lymphocytes with dicentrics

Shielding	Model	GCR	Trapped p+	Total
Naussica	LET	2.20×10^{-3}	2.19×10^{-3}	4.39×10^{-3}
Naussica	Track	2.78×10^{-3}	2.66×10^{-3}	5.44×10^{-3}
Lyulin	LET	2.23×10^{-3}	2.46×10^{-3}	4.69×10^{-3}
Lyulin	Track	2.76×10^{-3}	3.02×10^{-3}	5.78×10^{-3}
Mir-18 crew member	Experiment[a]			$6.4(\pm 2) \times 10^{-3}$

[a] Yang et al. (1997).

$$P_j(E) = \exp(-\sigma_j F) P(D\gamma) \tag{10}$$

where F is the particle fluence and the second factor in Eq. (10) represents the inter-track contribution using the dose fraction available to act through inter-track action. For low-dose rate exposures only the first factor in Eq. (10) contributes. Comparison of the track-structure model to the charged particle data are shown in Fig. 7. We note important differences between the two models shown in Figs. 6 and 7 in extrapolating away from the available data. It can be seen existing experimental cannot distinguish between these two models which employ vastly different assumptions. Extrapolations necessary over the radiation types and energies found in space must be considered tentative until the necessary data or predictive capabilities are in hand.

4. Comparisons to spaceflight measurements on Mir

We next compare calculations for the fraction of lymphocytes with dicentric aberrations to occur in astronauts on the Mir-18 mission (Yang et al., 1997). The Mir-18 mission had a duration of 115 days from March 2 through June 18, 1996 near solar minimum conditions. Calculations for the number of aberrations on the Mir-18 mission were made using particle energy distributions from the HZETRN which propagates the external environment through spacecraft shielding and body-self shielding and the biophysical models described above. The particle energy distributions are folded with biological response functions to determine the number of aberrations as

$$N_{\text{aber}} = \Sigma_s c_s \Sigma_j \int \mathrm{d}E \phi(x_s, E) R_j(E) \tag{11}$$

where the c_s represent the fractional contribution from a given shielding segment. We use the shielding distributions for the Naussica and Lyulin modules on the Mir in the comparisons described below. In our calculations we include the background-rate for dicentrics determined by Yang et al. (1997). We apply the biological response models using the relative biological effectiveness (RBE) to scale to the photon response curve for dicentrics measured by Yang et al. (1997). This is done to reduce the effects of variations in photon response between the in vitro data of Edwards et al. (1994) and Sasaki et al. (1998) and the in-vitro data of Yang et al. (1997) for the pre-flight lymphocyte response to photons from Mir crew members.

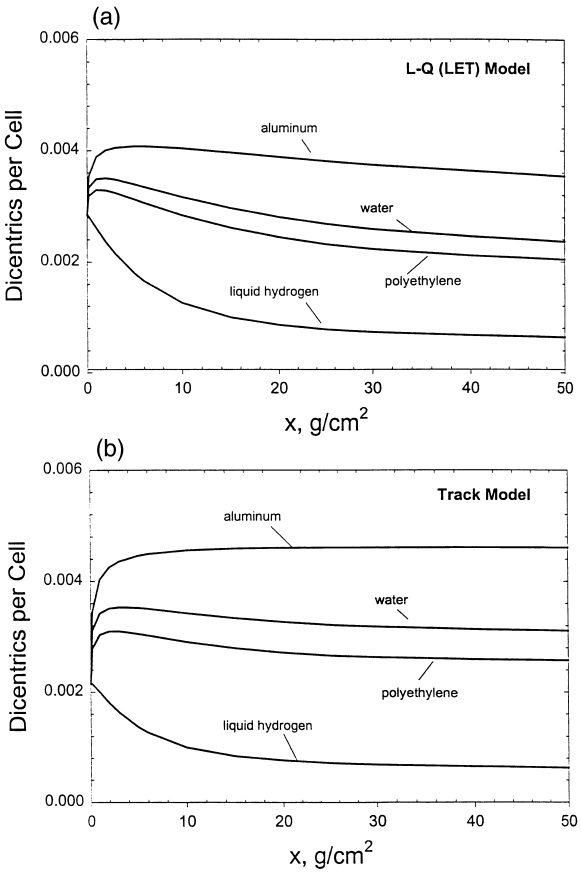

Fig. 8. The attenuation of the average number of dicentrics per cell from GCR with shielding depths predicted by biophysics for various materials. (a) L–Q LET model. (b) Track model.

Table 2 shows the integrated results after consideration of the Mir and astronaut shielding models. We have use the computerized anatomical man (CAM) model shield distribution for the blood forming organs to represent the shielding of the circulating lymphocyte cells. The track model and L–Q model are both within one standard deviation of the value determined by Yang et al. (1997). The trapped protons make-up about one-half of the risk for dicentric formation which is a larger value than seen for the equivalent dose.

In Fig. 8 we show the depth distribution for dicentric formation on the Mir from GCR using the L–Q model and the track-structure model for several materials. These results show that for both models, aluminum shielding provides no protective effects to the GCR. Water and polyethylene also show no protective effects until large amounts of shielding are used. Only liquid H2 shows a protective effect amongst the materials considered. Of note is the similarity in the depth response from GCR for dicentric formation in the track model to the dose response shown in Fig. 2a. In contrast, the depth response to GCR for dicentric formation in the L–Q model is similar to the attenuation seen for the equivalent dose shown in Fig. 2b. Table 3 shows the contributions from individual charges at the entrance depth and at 20 g/cm^2 of aluminum with body-self shielding (about the average value for the Mir station). The effects of neutrons are through their charged secondaries, such that the contributions from charges, $Z = 1$ and 2 are approximately one-half from neutrons. Table 3 shows that for the average shielding configuration, low charge and energy ions (LZE) dominate due to the absorption of the heavy ions by spacecraft or body shielding. Differences occur in the relative contributions of charge groups in the models under consideration. Fig. 9 shows the attenuation for different materials for dicentrics from trapped protons. For trapped proton response, the two models provide similar results because of the dominant role of primary or secondary protons.

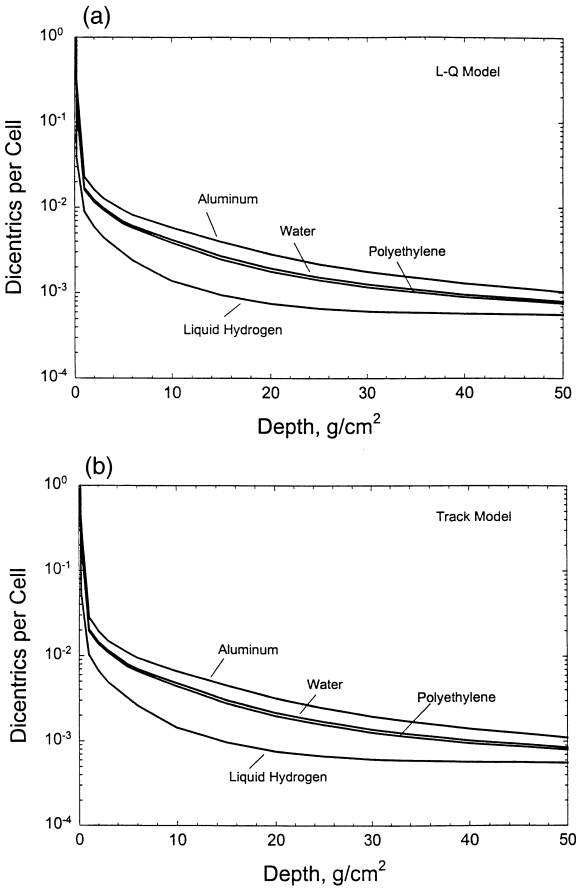

Fig. 9. The attenuation of the average number of dicentrics per cell from trapped protons with shielding depths predicted by biophysics model for various materials. (a) L–Q LET model. (b) Track model.

Table 3
A. Charge contributions to percent dose equivalent or dicentric formation with no shielding

Z	Equivalent dose	L–Q	Track
1	12.7%	9.6%	10.8%
2	3.4	2.8	3.5
3–9	6.8	32.6	14.0
10–16	23.8	31.7	28.8
17–23	14.7	7.7	11.8
24–28	38.6	15.6	31.1

B. Charge contributions to percent equivalent dose or dicentric formation with 20 g/cm^2 of aluminum shielding and body self-shielding

Z	Equivalent dose	L–Q	Track
1	35.8%	44.7%	49.2%
2	29.5	21.7	33.4
3–9	2.4	14.8	4.5
10–16	10.8	11.6	5.9
17–23	11.0	3.8	3.1
24–28	10.5	3.4	3.9

5. Discussion

The models described above are in good agreement with physical and biological dosimetry from the Mir-

18 mission. The comparison made for the attenuation of equivalent dose and the risk for dicentric formation indicate the poor characteristics of aluminum shielding for mitigating the effects of the GCR. Because of the dominant contributions from high-energy particles in LEO these effects are even larger than shown in previous calculations of the attenuation characteristics of the GCR in free space (Cucinotta et al., 1997; Letaw et al., 1989; Wilson et al., 1995). However, nominal amounts of shielding are indeed necessary in LEO to protect from the effects of trapped protons and electrons. Our study suggests that aluminum shielding with areal density above about 3–5 g/cm^2 provides little decrease in risk. This is primarily due to the increased effectiveness of low-energy and charge (LZE) particles of similar LET as high energy and charge (HZE) ions. If the models considered underestimate the biological effectiveness of low energy hydrogen and helium ions produced from nuclear collisions, then 3–5 g/cm^2 of aluminum shielding may in fact increase the radiological risk. Clearly, studies with more relevant endpoints than dicentrics are needed. Future studies should also consider alternative models of energy deposition (Charlton et al., 1989; Edwards et al., 1994).

There are many factors regarding biodosimetry comparisons that need to be considered for proper interpretation and for future model developments. Dicentrics are used as a convenient marker because they occur at a higher frequency and are easily scored in comparison to other aberration types (Edwards, 1997; Straume and Bender, 1997). A reasonable distribution of track segment irradiation have been made for dicentrics in human lymphocytes (Edwards, 1997; Edwards et al., 1994; Sasaki et al., 1998) allowing comparisons of biophysical models to the Mir-18 results. However, clearly more data are needed for understanding the complicated radiation field since behind spacecraft shielding in LEO. This is even more true for more relevant aberration types such as translocations (Solomon et al., 1991) or deletions. Here detailed measurements of the dose response for a large number of ion types have not been reported. Also, delayed aberrations that result from genomic instability, including chromatid aberrations, may be more relevant in cancer formation (Kadhim et al., 1995). In addition, there are questions of survivability related using dicentrics for prolonged exposures. Dicentrics are unstable aberrations and the loss of cells with time is a concern for the protracted exposures that occurred over the 115 days during Mir-18. Edwards (1997) reports a half-life for lymphocytes of 3 years, however a recent study by Matsumoto et al. (1998) showed a significant loss of dicentrics within the first week following irradiation with ^{137}Cs gamma rays at doses of 0.5–4 Gy. There are also issues related to dose-rate effects. These issues include the role of a sub-alpha response in the extrapolation of acute exposures to low-dose rates (Williams et al., 1999), adaptive responses (Sasaki, 1992), interphase cell death, G1 arrest, and the non-additivity of responses in mix-field irradiation (Cucinotta, 1999; Curtis, 1996; Virsik-Peuckert et al., 1997; Zaider and Dicello, 1978). Genetic factors in radiation responses also need to be considered (Virsik-Peuckert et al., 1997; Williams et al., 1999). Such factors will be discussed elsewhere.

Acknowledgements

This work was sponsored, in part, by the National Space Biomedical Research Institute (NSBRI).

References

Alt, F.W., Oltz, E.M., Young, F., Gorman, J., Taccioli, G., Chen, J., 1992. V(D)J recombination. Immunol. Today 13, 306–314.

Badhwar, G.D., Cucinotta, F.A., 1998. Depth dependence of absorbed dose, dose equivalent, and LET in polyethylene and comparison with model calculations. Radiation Research 149, 209–218.

Badhwar, G.D., Atwell, W., Cash, B., Ptrov, V.M., Akatov, Y.A., Tchernykh, I.V., Shurshakov, V.A., Arkhangelsky, V.A., 1998. Radiation environment on the MIR orbital station during solar minimum. Adv. Space. Res. 22, 501–510.

Belli, M., Cera, F., Cherubini, R., Haque, A.M.I., Ianzini, F., Moschini, G., Sapora, O., Simone, G., Tabocchini, M.A., Tiveron, P., 1993. Inactivation and mutation induction in V79 cells by low energy protons: re-evaluation of the results at the LNL facility. Int. J. Radiat. Biol. 63, 331–337.

Belli, M., Cera, F., Cherubini, R., Ianzini, F., Moschini, G., Sapora, O., Simone, G., Tabocchini, M.A., Tiveron, P., 1994. DNA double strand breaks induced by low energy protons in V79 cells. Int. J. Radiat. Biol. 65, 529–536.

Charlton, D.E., Nikjoo, H., Humm, J.L., 1989. Calculation of initial yields of single- and double strand breaks in nuclei from electrons, protons, and alpha particles. Int. J. Radiat. Biol. 56, 1–19.

Chen, A.M., Lucas, J.N., Simpson, P.J., Griffin, C.S., Savage, J.R.K., Brenner, D.J., Hlatky, L.R., Sachs, R.K., 1997. Computer simulation of data on chromosome aberrations produced by X rays or alpha particles and detected by fluorescence in situ hybridization. Radiat. Res. 148, S93–S101.

Cucinotta, F.A., 1999. Issues in risk assessment from solar particle events, Radiat. Meas. 30, 261–268.

Cucinotta, F.A., Wilson, J.W., Katz, R., Atwell, W., Badhwar, G.D., 1995. Track structure and radiation transport models for space radiobiology studies. Adv. Space Res. 18, (12183–(12)194.

Cucinotta, F.A., Wilson, J.W., Shinn, J.L., Badavi, F.F., Badhwar, G.D., 1996a. The effects of target fragmentation

on LET spectra from space radiation. Radiat. Meas. 26, 923–934.

Cucinotta, F.A., Wilson, J.W., Shavers, M.R., Katz, R., 1996b. Effects of track structure and cell inactivation on the calculation of heavy ion mutation rates in mammalian cells. Int. J. Radiat. Biol. 69, 593–600.

Cucinotta, F.A., Wilson, J.W. 1997. Assessment of current shielding issues. In: Shielding Strategies for Human Space Exploration. NASA CP 3360.

Cucinotta, F.A., Wilson, J.W., Shinn, J.L., Tripathi, R.K., 1998. Assessment and requirements of nuclear reaction data bases for GCR transport in the atmosphere and structures. Adv. Space. Res. 21, 1753–1762.

Curtis, S.B., 1996. Possible effects of protracted exposure on the additivity of risks from space radiations. Adv. Space. Res. 18, (12)41–(12)44.

Edwards, A.A., 1997. The use of chromosome aberrations in human lymphocytes for biological dosimetry. Radiat. Res. 148, S39–S44.

Edwards, A.A., Finnon, P., Moguet, J.E., Lloyd, D.C., Darroudi, F., Natarajan, A.T., 1994. The effectiveness of high energy neon ions in producing chromosomal aberrations in human lymphocytes. Radiat. Prot. Dos. 52, 299–303.

Friedberg, E.C., Walker, G.C., Siede, W., 1995. DNA repair and mutagenesis. ASM Press, Washington DC.

GOST, 1991. LET Dependence of Cosmic Radiation Quality. GOST 25645.218-90, Gosstandart SSSR, Moscow.

ICRP-26, 1976. Annals of the ICRP, 1976. Recommendations of the International Commission on Radiological Protection. ICRP Publication 26, Pergamon Press, Oxford.

ICRP-60, 1990. Annals of the ICRP, 1990. Recommendations of the International Commission on Radiological Protection. ICRP Publication 60, Pergamon Press, Oxford.

Kadhim, M.A., Lorimore, S.A., Townsend, K.M.S., Goodhead, D.T., Bucker, V.J., Wright, E.G., 1995. Radiation-induced genomic instability: delayed cytogenetic aberrations and apoptosis in primary human bone marrow cells. Int. J. Radiat. Biol. 57, 287–293.

Katz, R., Ackerson, B., Homayoonfar, M., Scharma, S.C., 1971. Inactivation of cells by heavy ion bombardment. Radiat. Res. 47, 402–425.

Kiefer, J., Schneider, E., 1994. Mutation induction by heavy ions. Adv. Space Res. 14, 257–265.

Letaw, J.R., Silberberg, R., Tsao, C.H., 1989. Radiation hazards on space missions outside the magnetosphere. Adv. Space Res. 9, (10285–(10)291.

Matsumoto, K., Ramsey, M.J., Nelson, D.O., Tucker, J.D., 1998. Persistence of radiation-induced translocations in human peripherial blood determined by chromosome painting. Radiat. Res. 149, 602–613.

Menz, R., Anders, R., Larsson, B., Ozsahin, M., Trott, K., Crompton, N.E.A., 1997. Biological dosimetry: the potential use of radiation-induced apoptotsis in human T-lymphocytes. Radiat. Env. Biophys. 36, 175–181.

Morgan, W.F., Day, J.P., Kaplan, M.I., McGhee, E.M., Limoli, C.L., 1996. Genomic instability induced by ionizing radiation. Radiat. Res. 146, 247–258.

NCRP, 1989. National Council on Radiation Protection and Measurements. Guidance on Radiation Received in Space Activities NCRP Report No. 98. National Council on Radiation Protection and Measurements, Bethesda, MD.

Nelson, W.G., Kastan, M.B., 1994. DNA strand breaks: the DNA template alterations that trigger p53-dependent DNA response pathways. Mol. Cell. Biol. 14, 1815–1823.

Nikjoo, H., O'Neill, P., Goodhead, D.T., Terissol, M., 1997. Computational modeling of low energy electron induced DNA damage by early physical and chemical events. Int. J. Radiat. Biol. 71, 467–483.

Obe, G., Johannes, I., Johannes, C., Hallman, K., Reitz, G., Facius, R., 1997. Chromosomal aberrations in blood lymphocytes of astronauts after long-term space flights. Int. J. Radiat. Biol. 72, 727–734.

Reed, M., et al., 1995. The C-terminal domain of p53 recognizes DNA damaged by ionizing radiation. Proc. Natl. Acad. Sci. USA 92, 9455–9459.

Resnick, M.A., 1976. The repair of double-stand breaks in DNA: a model involving recombination. Journal of Theoretical Biology 59, 97–106.

Revell, S.H., 1974. The breakage and reunion theory and the exchange theory for chromosome aberrations induced by ionizing radiations: a short history. Adv. Radiat. Biol. 4, 367–416.

Roth, D.B., Porter, T.N., Wilson, J.H., 1985. Mechanisms of nonhomologous recombination in mammalian cells. Molecular and Cellular Biology 5, 2599–2607.

Sachs, R.K., Brenner, D.J., Chen, A.M., Hahnfeldt, P., Hlatky, L.R., 1997. Intra-arm and interarm chromosome interchanges: tools for probing the geometry and dynamics of chromatin. Radiation Research 148, 330–340.

Sasaki, M.S., 1992. Cytogenetic biomonitoring of human radiation exposures: possibilities, problems, and pitfalls. J. Radiat. Res. 33, S44–S53.

Sasaki, M.S., Takatsuji, T., Ejima, Y., 1998. The F value cannot be ruled out as a chromsomal fingerprint of radiation quality. Radiat. Res. 150, 253–258.

Savage, J.R.K., 1989. The production of chromosome changes by radiation: an update of Lea (1946), Chapter V1, British J. Radiology 507–520.

Solomon, E., Borrow, J., Goddard, A.D., 1991. Chromosome aberrations and cancer. Science 254, 1153–1160.

Straume, T., Bender, M.A., 1997. Issues in cytogenetic biological dosimetry: emphasis on radiation environments in space. Radiation Research 148, S60–S70.

Testard, I., Ricoul, M., Hoffschir, F., Flury-Herard, A., Dutrillaux, B., Fedorenko, B., Gerasimenko, V., Sabatier, L., 1996. Radiation-induced chromosome damage in astronauts lymphocytes. Int. J. Radiat. Biol. 70, 403–411.

Thacker, J., Stretch, A., Stevens, M.A., 1979. Mutation and inactivation of cultured mammalian cells exposed to beams of accelerated heavy ions II. Chinese hamster V79 cells. Int. J. Radiat. Biol. 36, 137–148.

Velculescu, V.E., Zhang, L., Vogelstein, B., Kinzler, K.W., 1995. Serial analysis of gene expression. Science 270, 484–487.

Virsik-Peuckert, P., Rave-Frank, M., Langebrake, U., Schmidberger, H., 1997. Differences in the yields of dicentrics and reciprocal translocations observed in the chromosomes of irradiated human skin fibroblasts and blood lymphocytes from the same healthy individuals. Radiation Research 148, 209–215.

Williams, J.R., Zhou, H., Osman, M., Dillehay, L.E., Kavet, R., Cucinotta, F.A., Dicello, J.F., Zhang, Y., 1999. Predicting cancer rates in astronauts from animal carcinogenesis studies and cellular markers. Mutation Research (in press).

Wilson, J.W., Townsend, L.W., Schimmerling, W., Khandelwal, G.S., Khan, F., Nealy, J.E., Cucinotta, F.A., Simonsen, L.C., Norbury, J.W., 1991. Transport methods and interactions for space radiations, RP1257, NASA, Washington DC.

Wilson, J.W., Kim, M., Schimmerling, W., Badavi, F.F., Thibeault, S.A., Cucinotta, F.A., Shinn, J.L., Kiefer, R., 1995. Issues in space radiation protection: galactic cosmic rays. Health Physics 68, 50–58.

Yang, T.C., George, K., Johnson, A.S., Durante, M., Fedorenko, B.S., 1997. Biodosimetry results from space flight Mir-18. Radiat. Res. 148, S17–S23.

Zaider, M., Dicello, J.F., 1978. RBEOER: A Fortran Program for the Computation of RBE's, OER's, Survival Ratios and the Effects of Fractionation Using the Theory of Dual Radiation Action. LA-7196-MS Report, Los Alamos Scientific Laboratory, Los Alamos NM.